Enhancement of mechanical entanglement and asymmetric steering with coherent feedback

Rui Peng, Chengsong Zhao, Zhen Yang, Junya Yang, and Ling Zhou [*]
School of Physics, Dalian University of Technology, Dalian 116024, China

We propose a scheme to enhance entanglement and asymmetric steering between two mechanical oscillators in an optomechanical system with coherent feedback control. In the system, an optical cavity interacts with two mechanical oscillators and an auxiliary cavity whose output field is fed back into the input port of the optical cavity via a feedback loop. Due to the coherence between the auxiliary cavity and feedback, we derive the effective decay rate and a nonzero frequency shift of the optical cavity. Consequently, the induced beam-splitter-type and parametric-type interactions between the two mechanical oscillators are modulated, which leads to the enhancement of entanglement and the generation of asymmetric steering even if the two mechanical oscillators possess identical decoherence properties. And the direction of asymmetric steering can be controlled by tuning the jumping phase between two cavities and optimizing the ratio of drive asymmetry. In contrast to the method of adding losses or noises to one subsystem at the cost of reducing steerability, this scheme provides an active way to achieve enhanced asymmetric steering. Furthermore, the steady-state and dynamical entanglement and asymmetric steering can be generated in the unresolved-sideband regime, which is friendly for experimental implementation.

I. INTRODUCTION

Quantum entanglement recognized as the most intrinsic feature of quantum mechanics is a valuable resource for quantum information processing, such as performing computation and secure communication [1–3]. A great deal of effort has been devoted to generating and enhancing entanglement [4–13], especially for the entanglement between mechanical oscillators [14–16], because the mechanical oscillator possesses a long decoherence time and plays a key role in testing the validity of quantum mechanics [17] and probing decoherence theories [18,19]. However, the mechanical oscillator is easily sensible to the external force but cannot be directly detected. The optomechanical system, connecting the optical and mechanical modes via radiation pressure, is an ideal platform to detect the mechanical state [20–22] as well as to generate mechanical entanglement [23–26]. Based on the fact that entanglement is normally vulnerable to environmental noise, reservoir engineering [27–31] is an efficient avenue for obtaining a large degree of mechanical entanglement [15,24,32] by effectively modifying the dissipation of the mechanical oscillator in the optomechanical system. Recently, people have experimentally demonstrated macroscopic entanglement between two mechanical oscillators by explicitly using the dissipative nature of the microwave resonator [33–36].

Feedback control is an alternative way to enhance entanglement [37–42] by implementing the additional operation on the optical field via feedback loop where quantum information is extracted from the system and fed back into the system.

Depending on the presence of a measurement device in the feedback loop, there are two kinds of feedback control: one is the measurement-based feedback which involves the feedback of the classical information (e.g., the photocurrent) obtained by making a measurement on the system and makes the noise spectrum squashed or antisquashed [43,44]; the other is coherent feedback [45–47] involving the feedback of the quantum information via a full quantum loop without measurement. In the aspect of enhancing entanglement, coherent feedback does not introduce additional noise and has a significant advantage [39–42]. Especially, Li *et al.* has reported a scheme to reduce the optical decay rate via coherent feedback to enhance the mechanical entanglement with the cooling of one Bogoliubov mode [40].

On the other hand, Einstein-Podolsky-Rosen (EPR) steering, being a strict subset of entanglement [48,49], describes the effect of one particle via local measurement on the state of another in a pair of entangled particles. Such a one-side device-independence feature attracts considerable interests and is widely used in various quantum information protocols, for example, quantum secret sharing [50–52], one-way quantum computing [53], no-cloning quantum teleportation [54,55], and subchannel discrimination [56]. The feature of steering significantly distinguishing it from entanglement and nonlocality is the asymmetry, which indicates the different steerabilities in two opposite directions [57,58]. An important method to achieve asymmetric steering is to obtain asymmetric states by introducing different losses or noises to the subsystems, which is at the expense of correlation [50,58–60]. When the symmetric additional noise is introduced, the steering can be enhanced but lacks the asymmetry [37,38]. In contrast, the asymmetric steering can be achieved by introducing asymmetric additional noise with the cost of reducing

---

*[*] zhlhxn@dlut.edu.cn

steerability [38]. Therefore, we expect a method that can both improve the correlation of the system and manipulate the asymmetric steering without consuming correlation. Recently, a phase-control scheme based on the interference effect was proposed to manipulate and enhance the asymmetric steering in a closed-loop three-mode system [61]. In the general model, pairwise interactions between the three modes are required, which limits the applicability of the general model.

In this paper, we aim at the enhancement of entanglement and the manipulation of asymmetric steering between two mechanical oscillators in an auxiliary-cavity-assistant optomechanical system with coherent feedback control. In the system, the optical cavity interacting with two mechanical oscillators couples to an auxiliary cavity whose output field is fed back into the input port of the optical cavity via feedback loop. Under the joint effect of auxiliary cavity and feedback, the steady-state entanglement and steering can be enhanced significantly, which benefits from the modification of the induced beam-splitter and parametric-type interactions between two mechanical oscillators. Moreover, we show that the steady-state and dynamical entanglement and steering can be generated under the unresolved-sideband regime, which results from the reduction of the effective optical decay rate. And the enhanced dynamical entanglement and steering can reach steady values in a shorter time, because the induced interaction between two mechanical oscillators and mechanical damping rate are improved simultaneously. On the other hand, it is possible to obtain asymmetric steering between two mechanical oscillators possessing completely symmetric decoherence properties. And the direction of steering can be manipulated by modulating the jumping phase between cavities and optimizing the ratio of drive asymmetry.

This scheme significantly distinguishes from the method by introducing different amounts of losses or noises to the subsystems [59,60] which in general leads to the reduction of correlation. For the asymmetric steering of two mechanical oscillators induced by the interference effect, the phase-dependent beam-splitter-like interaction between two mechanical oscillators is required [61]. In our system, the phase belongs to the coupling of two cavity modes, which is more friendly for experimental implementation. Although the coherent feedback has been used in improving quantum entanglement in [40], manipulating asymmetric steering by jointing the coherent feedback and the jumping rate between two cavities in the current scheme is obviously different from [40]. In contrast to the method of manipulating asymmetric steering with measurement-based feedback [37,38], this scheme avoids the degradation of correlations because coherent feedback does not introduce additional noise to the system. Therefore, we demonstrate that there is a significant advantage of extending coherent feedback to manipulate the asymmetry of steering.

The remainder of this paper is organized as follows. In Sec. II, we first provide the Hamiltonian of the optomechanical system without feedback, and then we derive the modified quantum Langevin equations (QLEs) of the feedback-modified system. In Sec. III, we present the measure of quantum entanglement and Gaussian steering and show the numerical results of the enhanced entanglement and steering with the function of the auxiliary cavity and feedback. The
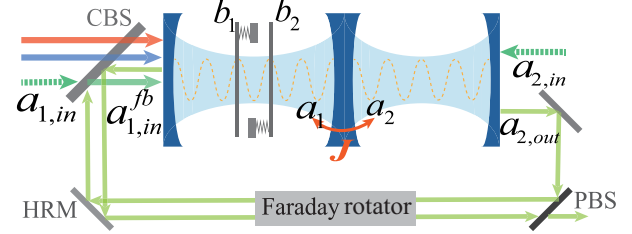

FIG. 1. Schematic diagram of the optomechanical system with feedback loop. The optical cavity a_1 driven by a pair of control lasers interacts with two mechanical oscillators b_1 and b_2. The cavity a_2 couples to cavity a_1 with strength J and phase θ. The output field of auxiliary cavity mode a_2 is fed back to the input port of the cavity mode a_1 through highly reflective mirrors (HRM) and a control beam splitter (CBS) with tunable reflectivity R. In the feedback loop, the Faraday rotator and polarization beam splitter (PBS) combine to prevent interference from reflections. $a_{1,\text{in}}$, $a_{2,\text{in}}$ denote the input vacuum noises for the cavities, and $a_{1,\text{in}}^{fb}$ is the new input field modified by feedback from the output field of cavity mode a_2.

experimental implementations of the system and the detection of entanglement are given in Sec. IV. Finally, we draw our conclusion in Sec. V.

II. MODEL

A. The system without feedback

As sketched in Fig. 1, the optomechanical system consists of two membranes acting as mechanical oscillators and two coupled cavities with resonant frequency ω_c, where the output field of the auxiliary cavity a_2 is sent to the input port of the other cavity a_1 via feedback loop. The cavity a_1 interacts with two mechanical oscillators with frequencies Ω_1 and Ω_2 and is driven by a pair of control lasers at frequency $\omega_c \pm \omega_d$ [$\omega_d = (\Omega_1 + \Omega_2)/2$], which allows the generation of entanglement between two mechanical oscillators. In the frame rotating with $H_0 = \sum_{j=1,2} \omega_c a_j^\dagger a_j$, the Hamiltonian of the system can be written as ($\hbar = 1$)

$$
\begin{aligned}
H = & \sum_{j=1,2} [\Omega_j b_j^\dagger b_j + g_j a_1^\dagger a_1 (b_j + b_j^\dagger)] \\
& + [Je^{i\theta} a_1^\dagger a_2 + iE(t)a_1^\dagger + \text{H.c.}].
\end{aligned}
\tag{1}
$$

a_j ($a_j^\dagger$) and b_j ($b_j^\dagger$) ($j = 1, 2$) refer to the annihilation (creation) operators of the jth cavity mode and the jth mechanical oscillator with the optical decay rate κ_j and the mechanical damping rate γ_j, respectively. $g_j = \omega_c/(L\sqrt{m_j\Omega_j})$ characterizes the single-photon coupling strength between the optical cavity a_1 and the mechanical oscillator b_j. The coupling strength between two cavities is J with phase θ. $E(t) = E_1 e^{i\omega_d t} + E_2 e^{-i\omega_d t}$ is the time-dependent amplitude of the control lasers where E_j is related to the input laser power P_j and defined by $E_j = \sqrt{2\kappa_j P_j/\omega_L}$. The dynamics of the system can be described by the QLEs:

$$
\begin{aligned}
\dot{a}_1 = & -\kappa_1 a_1 + \sqrt{2\kappa_1}a_{1,\text{in}} - i\sum_{j=1,2} g_j a_1(b_j + b_j^\dagger) \\
& - iJe^{i\theta} a_2 + E_1 e^{i\omega_d t} + E_2 e^{-i\omega_d t},
\end{aligned}
$$

$$\dot{a}_2 = -\kappa_2 a_2 + \sqrt{2\kappa_2}a_{2,\text{in}} - iJe^{-i\theta}a_1,$$
$$\dot{b}_j = -(\gamma_j + i\Omega_j)b_j + \sqrt{2\gamma_j}b_{j,\text{in}} - ig_j a_1^\dagger a_1, \qquad (2)$$

where o_{in} ($o = a_j, b_j$) is the input noise operator, with the nonzero correlation functions $\langle a_{j,\text{in}}(t)a_{j,\text{in}}^\dagger(t')\rangle = \delta(t - t')$, $\langle b_{j,\text{in}}^\dagger(t)b_{j,\text{in}}(t')\rangle = n_{j,\text{th}}\delta(t - t')$, and $\langle b_{j,\text{in}}(t)b_{j,\text{in}}^\dagger(t')\rangle = (n_{j,\text{th}} + 1)\delta(t - t')$. Here $n_{j,\text{th}} = [\exp(\hbar\Omega_j/k_B T) - 1]^{-1}$ is the mean thermal phonon number at the environment temperature T, and k_B is the Boltzmann constant. When cavity mode a_1 is driven by the strong classical fields and evolves to a large mean value, the standard linearization technique can be adopted with $o \to \langle o\rangle_s + \delta o$ ($o = a_j, b_j$), where $\langle o\rangle_s$ denotes the classical c-number mean value and δo represents quantum fluctuation around the classical mean value (for simplicity, the δ in δo is ignored in the following). In the weak optomechanical coupling regime, i.e., $|g_j/\Omega_j| \ll 1$, it is sufficient to consider the zeroth-order term of g_j for the classical mean values. In the long-time limit, we have

$$\langle a_1\rangle_s^{(0)} = \frac{E_1 e^{i\omega_d t} + E_2 e^{-i\omega_d t}}{\kappa_1 + \frac{J^2}{\kappa_2}},$$

$$\langle a_2\rangle_s^{(0)} = \frac{-iJe^{-i\theta}\langle a_1\rangle_s^{(0)}}{\kappa_2}, \quad \langle b_j\rangle_s^{(0)} = 0. \qquad (3)$$

The linearized Hamiltonian can be given by

$$H_{\text{lin}} = \sum_{j=1,2} \{\Omega_j b_j^\dagger b_j + [G(t)a_1^\dagger + G^*(t)a_1](b_j + b_j^\dagger)\}$$
$$+ J(e^{i\theta}a_1^\dagger a_2 + e^{-i\theta}a_2^\dagger a_1), \qquad (4)$$

where $g_{1,2} = g$ is assumed. $G(t) = g\langle a_1\rangle_s^{(0)} = G_1 e^{i\omega_d t} + G_2 e^{-i\omega_d t}$ with $G_{1,2} = gE_{1,2}/(\kappa_1 + \frac{J^2}{\kappa_2})$ is the effective optomechanical coupling. In the interaction picture with $H_0 = \sum_{j=1,2}\omega_d b_j^\dagger b_j$, the fast oscillating terms can be neglected under the rotating-wave approximation (RWA) when the condition $2\omega_d \gg \{G_1, G_2\}$ is satisfied, thus

$$H_{\text{RWA}} = \delta(b_1^\dagger b_1 - b_2^\dagger b_2) + J(e^{i\theta}a_1^\dagger a_2 + e^{-i\theta}a_2^\dagger a_1)$$
$$+ a_1^\dagger[G_1(b_1 + b_2) + G_2(b_1^\dagger + b_2^\dagger)] + \text{H.c.}, \qquad (5)$$

where the frequency difference of two mechanical oscillators is $\delta = (\Omega_1 - \Omega_2)/2$. From Eq. (5), it is clear that the two mechanical oscillators can be entangled because both are coupled with the cavity field. In view of the two-mode squeezed state, the cavity mode a_1 is used to cool the sum of Bogoliubov modes $\beta_{\text{sum}} = (b_1 + b_2)\cosh(r) + (b_1^\dagger + b_2^\dagger)\sinh(r)$ with the cooling rate $\sqrt{G_1^2 - G_2^2}$ and the squeezing parameter $r = \text{artanh}(G_2/G_1)$, and the ground states of a pair of Bogoliubov modes imply that two mechanical oscillators are in a two-mode squeezed state [15,24,34]. Therefore, there is a possible way to enhance the mechanical entanglement by modifying the effective decay rate and frequency shift of the cavity mode a_1. In the following subsection, we show the joint effects of coherent feedback and the auxiliary cavity a_2 on the cavity mode a_1 and thus the modifications of the effective mechanical damping rate and interactions between two mechanical oscillators.

B. The feedback-modified system

We now analytically analyze the effect of feedback control on the two mechanical oscillators in the limit of instantaneous feedback. The coherent feedback loop is applied to construct the unidirectional coupling between the source system with the auxiliary cavity, where unidirectivity can be achieved by using a Faraday rotator and polarization-sensitive beam splitters [45,62]. The feedback channel sends the output field of cavity a_2 to the input port of cavity a_1, and the output of the cavity mode a_1 cannot reflect into the auxiliary cavity a_2 with the assistance of unidirectional coupling. According to the standard input-output relation, the output field $a_{2,\text{out}}$ can be obtained as $a_{2,\text{out}} = \sqrt{2\kappa_2}a_2 - a_{2,\text{in}}$, and then the new input field of cavity a_1 is the superposition of the original input field $a_{1,\text{in}}$ and the output field $a_{2,\text{out}}$. By mixing the two fields in a beam splitter, the input field modified by the feedback is

$$a_{1,\text{in}}^{\text{FB}} = Ta_{1,\text{in}} + Ra_{2,\text{out}}, \qquad (6)$$

where T and R are the transmission and reflectivity, respectively, with $T^2 + R^2 = 1$ for a beam splitter without absorption. Due to the loss in the feedback channel, the perfect reflection cannot be realized, i.e., $0 \leqslant R < 1$. The original input noise operator $a_{1,\text{in}}$ is replaced by $a_{1,\text{in}}^{\text{FB}}$ and then we can find the modified QLE of the cavity mode a_1:

$$\dot{a}_1 = -\kappa_1 a_1 + (-iJe^{i\theta} + 2R\sqrt{\kappa_1\kappa_2})a_2$$
$$- i[G_1(b_1 + b_2) + G_2(b_1^\dagger + b_2^\dagger)]$$
$$+ \sqrt{2\kappa_1}(Ta_{1,\text{in}} - Ra_{2,\text{in}}). \qquad (7)$$

Comparing the second equation of (2) with Eq. (7), it is clear that the one-way feedback contributes an asymmetric coupling between two optical modes with strength $2iR\sqrt{\kappa_1\kappa_2}$. In order to find the effect of the jumping between two cavities and feedback, we can mathematically eliminate mode a_2 in the frequency domain. The Fourier transform of the operator is defined by $o(\omega) = \frac{1}{\sqrt{2\pi}}\int_{-\infty}^{\infty} o(t)e^{i\omega t}dt$. In the frequency domain, plugging the second equation of Eqs. (2) into Eq. (7), then the modified dynamical equation of cavity mode a_1 is

$$\chi_a(\omega)a_1(\omega) = -i\sum_{j=1,2}[G_1 b_j(\omega) + G_2 b_j^\dagger(-\omega)] + \sqrt{2\kappa}A_{\text{in}}(\omega). \qquad (8)$$

Here, $\kappa_1 = \kappa_2 = \kappa$ is assumed. The optical input noise is modified as $A_{\text{in}}(\omega) = Ta_{1,\text{in}}(\omega) + \tilde{R}_\omega a_{2,\text{in}}(\omega)$, where the modified reflectivity is $\tilde{R}_\omega = R_{\text{mod}}(\omega) - R$ with $R_{\text{mod}}(\omega) = \frac{2R\kappa - iJe^{i\theta}}{-i\omega + \kappa}$. The optical susceptibility is defined by $\chi_a(\omega) = -i\omega + \kappa + \chi_{\text{FB}}(\omega)$, where $\chi_{\text{FB}}(\omega) = \frac{J^2 + 2i\kappa JRe^{-i\theta}}{-i\omega + \kappa} = (iJe^{-i\theta})R_{\text{mod}}(\omega)$ arises from the auxiliary cavity and coherent feedback. In the resonant condition, we can obtain the effective decay rate $\kappa_{\text{eff}} = \kappa + \text{Re}[\chi_{\text{FB}}(0)]$ and frequency shift $\Delta_{\text{eff}} = \text{Im}[\chi_{\text{FB}}(0)]$ of the cavity mode a_1, which are given by

$$\kappa_{\text{eff}} = \kappa[1 + J^2/\kappa^2 + 2R\sin(\theta)J/\kappa],$$
$$\Delta_{\text{eff}} = 2JR\cos(\theta). \qquad (9)$$

Therefore, the modified optical susceptibility can be further simplified as $\chi_a(\omega) = \kappa_{\text{eff}} - i(\omega - \Delta_{\text{eff}})$. From Eqs. (9), it is clear that the feedback and the jumping between cavities are jointed together to modulate the loss of cavity a_1 and induce

an effective frequency shift. We will show that the effective decay rate κ_{eff} can be reduced, and the effective detuning can induce an effective parametric-type coupling between two mechanical oscillators.

To clearly show the dynamical equations of two mechanical oscillators under the effect of κ_{eff} and Δ_{eff}, we can eliminate optical modes in the frequency domain. Then we have

$$\chi_1(\omega)b_1(\omega) = \Lambda_1(\omega)b_2(\omega) + \Lambda_2(\omega)[b_1^\dagger(-\omega) + b_2^\dagger(-\omega)]$$
$$+ \sqrt{2\gamma}b_{1,\text{in}}(\omega) + B_{\text{in}}(\omega),$$

$$\chi_2(\omega)b_2(\omega) = \Lambda_1(\omega)b_1(\omega) + \Lambda_2(\omega)[b_1^\dagger(-\omega) + b_2^\dagger(-\omega)]$$
$$+ \sqrt{2\gamma}b_{2,\text{in}}(\omega) + B_{\text{in}}(\omega), \quad (10)$$

where the optical noise term is $B_{\text{in}}(\omega) = -i\sqrt{2\kappa}[\frac{G_1}{\chi_a(\omega)}A_{\text{in}}(\omega) + \frac{G_2}{\chi_a^*(-\omega)}A_{\text{in}}^\dagger(-\omega)]$. The effective coupling coefficients are $\Lambda_1(\omega) = \frac{G_2^2}{\chi_a^*(-\omega)} - \frac{G_1^2}{\chi_a(\omega)}$ and $\Lambda_2(\omega) = G_1 G_2(\frac{1}{\chi_a^*(-\omega)} - \frac{1}{\chi_a(\omega)})$. Plugging the modified optical susceptibility $\chi_a(\omega)$ into $\Lambda_1(\omega)$ and $\Lambda_2(\omega)$, then we can obtain

$$\Lambda_1(\omega) = \frac{(\kappa_{\text{eff}} - i\omega)(G_2^2 - G_1^2) + i\Delta_{\text{eff}}(G_1^2 + G_2^2)}{(\kappa_{\text{eff}} - i\omega)^2 + \Delta_{\text{eff}}^2},$$

$$\Lambda_2(\omega) = \frac{2i\Delta_{\text{eff}}G_1 G_2}{(\kappa_{\text{eff}} - i\omega)^2 + \Delta_{\text{eff}}^2}. \quad (11)$$

From Eqs. (10), we know that $\Lambda_1(\omega)$ and $\Lambda_2(\omega)$ respectively express the effective beam-splitter-type and parametric-type interactions between the two mechanical oscillators, both of which are dependent on the modified κ_{eff} and Δ_{eff}. Interestingly, the parametric-type interaction exists only when the nonzero optical frequency shift is induced. As we all know, the parametric-type interaction is beneficial for the generation of entanglement, therefore the nonzero optical frequency shift will support the enhancement of entanglement. On the other hand, the mechanical susceptibilities in Eqs. (10) are defined by $\chi_1(\omega) = -i\omega + i\delta + \gamma - \Lambda_1(\omega)$ and $\chi_2(\omega) = -i\omega - i\delta + \gamma - \Lambda_1(\omega)$, respectively. It can be found that the effective mechanical damping rate (Re$[\chi_{1,2}(\omega)]$) is $\Gamma = \gamma - \text{Re}[\Lambda_1(\omega)]$, and the effective mechanical frequency shifts are $\delta_1 = \delta + \delta_0$ (corresponding to mode b_1) and $\delta_2 = -\delta + \delta_0$ (corresponding to mode b_2), where $\delta_0 = -\text{Im}[\Lambda_1(\omega)]$ represents the induced mechanical detuning. Then, the free Hamiltonian, in addition to $\delta(b_1^\dagger b_1 - b_2^\dagger b_2)$, is added, $\delta_0(b_1^\dagger b_1 + b_2^\dagger b_2)$, which plays a key role in the manipulation of asymmetric steering.

III. ENTANGLEMENT AND STEERING

A. The measure of entanglement and steering

The quantum properties of the system can be obtained through the fluctuations of operators around the mean values. If the initial state is the Gaussian state, the system governed by the linearized Hamiltonian is still Gaussian. The properties of the system are fully represented by a 8×8 covariance matrix σ with elements defined as $\sigma_{mn} = \langle U_m U_n + U_n U_m \rangle/2$, where U_m is the mth row of the vector U defined by $U = [X_{a_1}, P_{a_1}, X_{a_2}, P_{a_2}, X_{b_1}, P_{b_1}, X_{b_2}, P_{b_2}]^T$, and the posi-

tion and momentum quadratures of the bosonic modes $o = a_j, b_j$ are $X_o = (o + o^\dagger)/\sqrt{2}$, $P_o = (o - o^\dagger)/(\sqrt{2}i)$. According to the Hamiltonian Eq. (4) and introducing the feedback Eq. (6), the dynamical QLEs can be written with a compact form as $\dot{U} = M(t)U + N$, where the drift matrix $M(t)$ and the vector of input noise N are given by Eqs. (A1) and (A3), respectively. Then we can derive a linear differential equation for the covariance matrix σ:

$$\dot{\sigma} = M(t)\sigma + \sigma M(t)^T + D, \quad (12)$$

where D is a diffusion matrix given by Eq. (A5). The components of D are defined as

$$D_{mn}\delta(t - t') = \langle N_m(t)N_n(t') + N_n(t')N_m(t)\rangle/2. \quad (13)$$

Here N_m is the mth row of the vector N. The steady-state covariance matrix σ can be obtained straightforwardly by solving the Lyapunov equation $M_0\sigma + \sigma M_0^T + D = 0$, where the time-independent drift matrix M_0 is given by Eq. (A2). According to the Routh-Hurwitz criterion [63], the system is stable when all eigenvalues of drift matrix M_0 have negative real parts. The stability condition is carefully checked in all simulations throughout this paper.

For the continuous-variable two-mode Gaussian state, it is convenient to use logarithmic negativity E_N [64,65] to measure the mechanical entanglement. In order to signify EPR steering, we adopt the measure of steering proposed in [66] for arbitrary bipartite Gaussian states. All measures mentioned above can be computed from the reduced covariance matrix V_{12} for two mechanical oscillators:

$$V_{12} = \begin{bmatrix} v_1 & v_{12} \\ v_{12}^T & v_2 \end{bmatrix}, \quad (14)$$

where v_1, v_2, and v_{12} are 2×2 sub-block matrices and can be extracted from the covariance matrix σ and given by $v_1 = \begin{bmatrix} \sigma_{55} & \sigma_{56} \\ \sigma_{65} & \sigma_{66} \end{bmatrix}$, $v_2 = \begin{bmatrix} \sigma_{77} & \sigma_{78} \\ \sigma_{87} & \sigma_{88} \end{bmatrix}$, and $v_{12} = \begin{bmatrix} \sigma_{57} & \sigma_{58} \\ \sigma_{67} & \sigma_{68} \end{bmatrix}$. Then the logarithmic negativity E_N and Gaussian steering S_{ij} in the direction from mode b_j to mode b_i are expressed as

$$E_N = \max[0, -\ln(2\eta^-)],$$
$$S_{12} = \max[0, \mathcal{R}(2v_2) - \mathcal{R}(2V_{12})],$$
$$S_{21} = \max[0, \mathcal{R}(2v_1) - \mathcal{R}(2V_{12})], \quad (15)$$

where $\eta^- = \frac{1}{\sqrt{2}}\sqrt{\Sigma - \sqrt{\Sigma^2 - 4\det(V_{12})}}$, $\Sigma = \det(v_1) + \det(v_2) - 2\det(v_{12})$, and $\mathcal{R}(w) = \frac{1}{2}\ln[\det(w)]$ is the Rényi-2 entropy. The larger values of E_N and S_{ij} imply the stronger entanglement and steerability.

B. The enhanced entanglement and asymmetric steering

In the subsection, we numerically show the enhancement of entanglement and the manipulation of asymmetric steering through jointing effect of the auxiliary cavity and coherent feedback.

From Eqs. (9), we know that the effective optical decay rate is enhanced when $\sin(\theta) > 0$, i.e., $\kappa_{\text{eff}} > \kappa$. In the following numerical calculation, we mainly focus on the condition $\sin(\theta) < 0$. In Fig. 2(a), we plot the dependence of entanglement E_N on jumping rate J and reflectivity R for $\theta = 1.5\pi$.
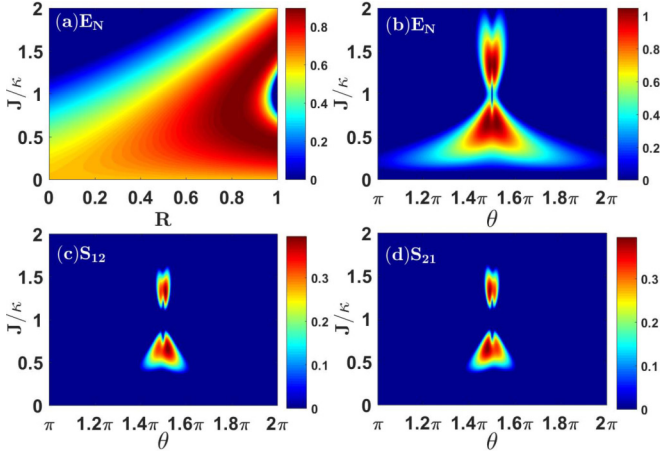
FIG. 2. (a) The steady-state entanglement E_N as a function of jumping rate J and reflectivity R when $\theta = 1.5\pi$ and $G_2/G_1 = 0.68$. The entanglement (b) and steering (c, d) as functions of jumping rate J and phase θ when $R = 0.99$ and $G_2/G_1 = 0.92$. The other parameters are $G_1/\Omega_1 = 0.1, \delta/\Omega_1 = 0.03, \kappa/\Omega_1 = 0.5, \gamma/\Omega_1 = 5 \times 10^{-6}$, and $n_{\text{th}} = 350$.
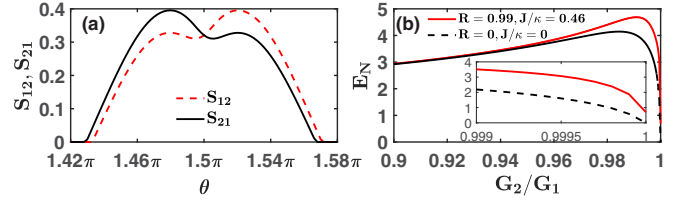

FIG. 3. (a) The steering $S_{12}(S_{21})$ as functions of the phase θ for $n_{\text{th}} = 350, G_2/G_1 = 0.92, R = 0.99, J/\kappa = 0.66$. (b) The entanglement E_N with (red solid curve) and without (black dotted curve) the auxiliary cavity and feedback vs drive asymmetry G_2/G_1 for $n_{\text{th}} = 0$ and $\theta = 1.48\pi$. The other parameters are the same as those in Fig. 2.

In this case, we have $\Delta_{\text{eff}} = 0$, and the effective interaction between two mechanical oscillators is only of beam-splitter form with coupling coefficient $\Lambda_1(\omega) = (G_2^2 - G_1^2)/(\kappa_{\text{eff}} - i\omega)$. When we fix the drive asymmetry G_2/G_1, the entanglement is manipulated only by the effective optical decay rate $\kappa_{\text{eff}} = \kappa[1 + \frac{J}{\kappa}(\frac{J}{\kappa} - 2R)]$. It is obvious that the entanglement can be enhanced owing to the introduction of auxiliary cavity and feedback. However, there is a significant degradation of entanglement around $R \to 1$ and $J = 1$, where $\kappa_{\text{eff}} \to 0$ and then $\Lambda_1(\omega)$ increases. The enhanced coupling strength $\Lambda_1(\omega)$ can improve the entanglement, but meanwhile the increased effective mechanical damping rate $\Gamma = \gamma - \text{Re}[\Lambda_1(\omega)]$ is harmful to entanglement. The competition between the two contrary factors results in the degradation of entanglement. That is, the entanglement does not increase monotonically with the decreasing of κ_{eff}. For the ideal reflectivity $R \to 1$, the effective optical decay rate can be simplified as $\kappa_{\text{eff}} = \kappa(\frac{J}{\kappa} - 1)^2$. When J/κ varies from 0 (2) to 1, κ_{eff} decreases monotonically, thus the entanglement is enhanced first and then degraded.

Aiming at revealing the effect of frequency shift Δ_{eff}, we plot entanglement in Fig. 2(b) and steering in Figs. 2(c) and 2(d) as functions of jumping rate J and phase θ. From Fig. 2(b), it is obvious that the entanglement cannot achieve its local maximum value at $\theta = 1.5\pi$, especially $J/\kappa \in [0.94, 1.06]$, where the entanglement is absent. This is because $\Delta_{\text{eff}} = 0$ for $\theta = 1.5\pi$, the effective interaction between two mechanical oscillators is only of beam-splitter form, and the parametric form coupling is zero. The optimal entanglement is achieved around $\theta = 1.48\pi, 1.52\pi$ and $J/\kappa = 0.66, 1.33$ where $\Delta_{\text{eff}} \neq 0$. The results mean that the entanglement can be enhanced with the help of the nonzero frequency shift. From Eqs. (11), both beam-splitter-type and parametric-type interactions are dependent on Δ_{eff}, so the entanglement can be improved by inducing a nonzero frequency shift Δ_{eff}. As shown in Figs. 2(c) and 2(d), though the two mechanical oscillators have identical decoherence properties

$\gamma_1 = \gamma_2 = \gamma$, $n_{1,\text{th}} = n_{2,\text{th}} = 350$, it is striking that the asymmetric steering can be achieved by tuning the phase of the jumping between cavities, such as for the same jumping rate $J/\kappa = 0.66$, $S_{12} > S_{21}$ when $\theta = 1.52\pi$ and $S_{12} < S_{21}$ when $\theta = 1.48\pi$. The asymmetric steering is strongly dependent on the phase due to Δ_{eff} affected by θ when the other parameters are settled.

To further study the key ingredient of the asymmetric steering in the system, we plot the dependence of them on the phase θ in Fig. 3(a). It can be found that at $\theta = 1.5\pi$, $\Delta_{\text{eff}} = 0$, then $S_{12} = S_{21}$, which means that the asymmetric steering only can be achieved with $\Delta_{\text{eff}} \neq 0$. The asymmetric steering requires a certain coherence condition between jumping and feedback. For $\Delta_{\text{eff}} \neq 0$, $\delta_0 = -\text{Im}[\Lambda_1(\omega)]$ can be induced so that the unequal effective mechanical frequency shifts $|\delta_1| \neq |\delta_2|$ are satisfied. Furthermore, the system modified by the feedback can realize the one-way steering which provides security in one-sided device-independent quantum key distribution. For example, when $\theta = 1.43\pi$, there only exists the one-way steering from mode b_1 to mode b_2, i.e., $S_{12} = 0$ and $S_{21} \neq 0$; in the opposite direction, the one-way steering from mode b_2 to mode b_1 can be achieved with $\theta = 1.57\pi$. Comparing with the way to manipulate asymmetric steering by adding asymmetric losses or noises to the subsystems, this method has a significant advantage of avoiding the degradation of correlation.

As we have presented in Eqs. (11), the effective interactions between two mechanical oscillators are related to the ratio G_2/G_1 when the effective optical decay rate κ_{eff} and frequency shift Δ_{eff} are fixed. It is necessary to reveal the dependence of entanglement on drive asymmetry shown in Fig. 3(b). Apparently, whether or not the auxiliary cavity and feedback are introduced, there is always an optimal drive asymmetry that maximizes the entanglement, which is resulted from the nonmonotonic dependence of the interactions $\Lambda_1(\omega)$ and $\Lambda_2(\omega)$ between the two mechanical oscillators on G_2/G_1. Interestingly, the entanglement can be achieved by introducing auxiliary cavity and feedback when $n_{\text{th}} = 0$ and $G_2 = G_1$ [see the inset in Fig. 3(b)]. The result is different from that case without the auxiliary cavity and feedback [24,60], where the mechanical entanglement is absent for the symmetric drive $G_2 = G_1$, because the optical mode fails to cool the Bogoliubov modes composed of the two mechanical oscillators. From Eqs. (11), when $G_2 = G_1$, we can find that there is no effective interaction between two mechanical oscillators for the case $J = 0$ and $R = 0$. If $J \neq 0$ and $R \neq 0$,
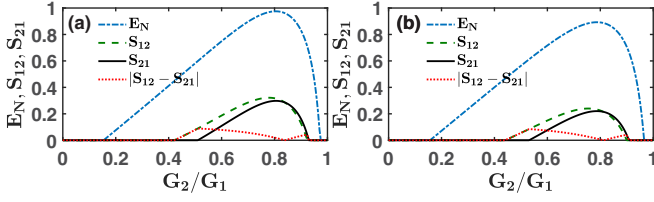
FIG. 4. The entanglement and steering as functions of drive asymmetry G_2/G_1 for different optical decay rates: (a) $\kappa/\Omega_1 = 0.5$, $J/\kappa = 0.46$, $\theta = 1.4\pi$; (b) $\kappa/\Omega_1 = 2$, $J/\kappa = 0.72$, $\theta = 1.48\pi$, $n_{th} = 350$.

thanks to the nonzero effective frequency shift of optical mode $\Delta_{eff} \neq 0$, the beam-splitter and parametric-type interactions between two mechanical oscillators emerge enabling strong entanglement under two symmetric classical drivings. In our simulation, we find that the entanglement is extremely fragile to the thermal noise when the system with feedback is driven by two tones with the same amplitudes. That is the reason why we choose $n_{th} = 0$ for Fig. 3(b).

Considering that the effective optical decay rate can be reduced due to the introduction of auxiliary cavity and feedback, we expect to relax the requirement for optical quality factor $Q = \omega_c/\kappa$. In Fig. 4, we plot the dependence of steady-state entanglement and steering on G_2/G_1 for different optical decay rates. Whether in the regime of resolved or unresolved sideband, the strong entanglement and steering can be achieved with the help of auxiliary cavity and feedback. From Figs. 4(a) and 4(b), we find that the overall asymmetry of steering is stepwise driven through the no-way regime ($S_{12} = S_{21} = 0$), one-way regime ($S_{12} \neq 0$ and $S_{21} = 0$), two-way regime ($S_{12} \neq 0$ and $S_{21} \neq 0$), one-way regime ($S_{12} = 0$ and $S_{21} \neq 0$), and no-way regime with the increase of ratio G_2/G_1. The dependence of steering on G_2/G_1 also can be explained by the dependence of $\Lambda_1(\omega)$ on G_2/G_1, because $\Lambda_1(\omega)$ is related with the induced mechanical oscillator $\delta_0 = -\text{Im}[\Lambda_1(\omega)]$ that results in the asymmetry of steering. Therefore, we can manipulate the asymmetry of steering by modulating the classical drivings when the asymmetric steering exists.

We show the entanglement and steering as functions of the thermal phonon number n_{th} displayed in Fig. 5. It is found that E_N is robust against the thermal phonon number where n_{th} can
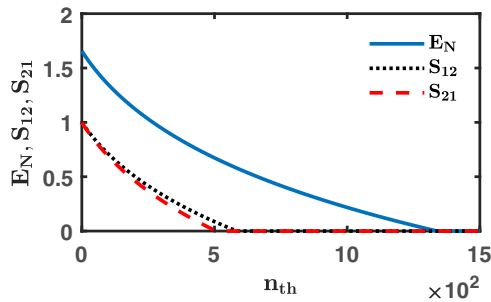

FIG. 5. The entanglement and steering of the system with the auxiliary cavity and feedback $R = 0.99$, $J/\kappa = 0.46$, $\theta = 1.4\pi$ as functions of the thermal phonon number n_{th} for a certain drive asymmetry $G_2/G_1 = 0.68$.
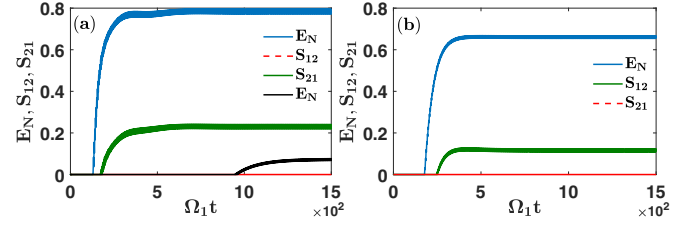

FIG. 6. Time evolution of entanglement and steering between two mechanical oscillators for the different optical decay rates. (a) In the resolved-sideband regime $\kappa/\Omega_1 = 0.316$, $(J/\kappa, R, G_2/G_1, \theta) = (0, 0, 0.5, 0)$ are chosen to plot the black solid curve. The other curves correspond to the modified system with parameters $(J/\kappa, R, G_2/G_1, \theta) = (0.75, 0.99, 0.88, 1.3\pi)$. (b) In the unresolved-sideband regime $\kappa/\Omega_1 = 2$, the relevant parameters are fixed as $(J/\kappa, R, G_2/G_1, \theta) = (0.85, 0.99, 0.85, 1.47\pi)$. The other parameters are $\gamma/\Omega_1 = 1.1 \times 10^{-5}$, $\delta/\Omega_1 = 0.158$, $G_1/\Omega_1 = 0.047$, $n_{th} = 85$.

be as large as 1300 and the steering S_{12}, S_{21} can survive even if $n_{th} = 500$. For a mechanical oscillator with resonant frequency $\omega/2\pi = 400$ kHz in the two-membrane-in-the-middle optomechanical system [67], the entanglement and steering can survive at the bath temperature $T \approx 24.96$ and 9.60 mK for $n_{th} = 1300$ and 500, respectively. Moreover, in the superconducting microcircuit [36], the mechanical oscillator with frequency $\omega/2\pi = 9.032$ MHz is fabricated, such that the thermal phonon number n_{th} of 1300 and 500 correspond to the bath temperature of $T \approx 563.7$ and 216.9 mK, respectively.

As for the dynamical entanglement and steering, in Fig. 6, we plot the time evolution of entanglement and steering for different optical decay rates κ. To get closer to the experiment, we choose the parameters from the experimental work [35], where the microwave optomechanical system consists of two aluminum drums embedded into a single microwave resonator. The decay rate of the cavity is $\kappa/2\pi = 800$ kHz, two mechanical oscillators process frequencies $\Omega_1 = 15.898$ MHz and $\Omega_2 = 10.865$ MHz, and mechanical decay time $1/\gamma_1 = 5.8$ ms and $1/\gamma_2 = 6.9$ ms. The two effective electromechanical couplings are $G_1 = 82 \times 2\pi$ kHz and $G_2 = 94 \times 2\pi$ kHz and the experimental parameters are measured at a temperature 7 mK. In Fig. 6(a), by comparing black and blue curves which correspond to the systems with and without auxiliary cavity and feedback, respectively, we can find that the dynamical entanglement is not only enhanced but also reaches the steady values in a shorter time due to introducing the auxiliary cavity and feedback. This result can be explained by the increasing of beam-splitter and parametric-type coupling strength and by the enhancing of the effective mechanical damping rate $\Gamma = \gamma - \text{Re}[\Lambda_1(\omega)]$ {$\text{Re}[\Lambda_1(\omega)] < 0$}. Without auxiliary cavity and feedback, the steering does not exist in the system. In the unresolved-sideband regime (e.g., $\kappa/\Omega_1 = 2$), the entanglement and steering do not exist when $R = 0$. By introducing the auxiliary cavity and feedback, the effective optical decay rate is reduced and the effective mechanical parametric-type interaction is induced yielding the presence of the entanglement and steering as shown by the curve in Fig. 6(b). In a word, the scheme supports the generation of the dynamical entanglement and

steering in the unresolved-sideband regime by the modulation of jumping rate between cavities and reflectivity, which is advantageous for the experimental implementation.

IV. EXPERIMENTAL IMPLEMENTATIONS

In this section, we discuss experimental realizations of the current scheme and the entanglement measures.

By inserting two separated membranes inside a Fabry-Pérot cavity, the two-membrane-in-the-middle cavity optomechanical system is realized [67–72]. Based on the device [67–72], if it is possible to introduce an auxiliary cavity and coherent feedback, and the present scheme can be constructed. The optomechanical coupling strength G_1 and G_2 can be manipulated by controlling the membrane position along the cavity axis [69,73–75]. For the jumping between two Fabry-Pérot cavities, a feasible implementation is to manipulate the reflectivity of the common mirror between the two cavities to tune the strength of coupling [76]. The phase of the jumping rate is controllable by tuning the phase of the driving lasers [77]. In addition, the beam-splitter-type interaction between two cavities also can be realized directly by the beam splitter with the relative phase θ [78]. Furthermore, we present a scheme to derive the complex coupling between two Fabry-Pérot cavities, as shown in Appendix B. The phase of the complex coupling is inherited from the classical field and can be controllable [79]. We assume an instantaneous feedback in this scheme because the feedback delay time is small enough to be ignored, e.g., for a 10-cm feedback loop, the delay time is 10^{-10} s. If the distance of light propagation in the feedback loop is so long that the delay is not negligible, one can cancel the effect of delay by imprinting a phase on light in the feedback loop [80].

Recently, the macroscopic entanglement between two micromechanical oscillators has been experimentally observed in the superconducting microcircuit [34–36]. The microwave optomechanical device consists of the superconducting transmission-line resonator and the mechanical drum-type oscillator. Compared with the dielectric membrane in the membrane-in-the-middle cavity optomechanical system, the drum has a higher frequency, such as in [36], and the two mechanical oscillators made of lithographically patterned thin-film aluminum that forms drumlike membranes are of frequencies $\Omega_1/2\pi = 6.692$ MHz and $\Omega_2/2\pi = 9.032$ MHz. For a certain thermal phonon number $n_{\text{th}} = [\exp(\hbar\Omega_j/k_B T) - 1]^{-1}$, the mechanical oscillator with higher frequency can put up with the higher bath temperature, therefore the entanglement and steering can be more robust against the bath temperature which is helpful to reduce the complexity of the experimental setups. In addition, with the help of the time-dependent exchange coupling [81–84] (the detailed derivation is given in Appendix B) or the phase shifter [85], the complex coupling between two superconducting microwave cavities can be realized. Coherent feedback has been realized in the superconducting circuits to produce the superconducting microwave multivibrator [86], in which two Kerr cavities are coherently coupled to each other in a loop via a beam splitter and display both bistable and astable dynamics. These researches support the experimental implementation of our scheme in the microwave optomechanical device.

As to the detection and verification of the mechanical entanglement and steering, whether with logarithmic negativity or Duan's inseparability criterion [87], one needs to measure the elements of reduced covariance matrix V_{12}, as used in [88]. One cannot directly measure the quadrature of the mechanical oscillator but can resort to the additional "probe" cavity mode, whose probe field is so weak that its effect on the mechanical oscillator can be negligible. When the detuning between the probe field and "probe" cavity mode is resonant with the mechanical oscillator, the beam-splitter-like interaction between "probe" cavity mode and mechanical oscillator is activated. And then in principle, all of the elements of matrix V_{12} can be obtained by measuring the correlation between two output fields of the "probe" cavity mode at the mechanical frequencies.

V. CONCLUSION

We have studied the enhancement of entanglement and the manipulation of steering between two mechanical oscillators in an auxiliary-cavity-assisted optomechanical system with coherent feedback. Due to introducing an auxiliary cavity and coherent feedback, the effective decay rate and frequency shift of the cavity mode are modulated. Consequently, the induced beam-splitter-type and parametric-type interactions between two mechanical oscillators are modified by the jumping rate between cavities as well as feedback parameter. When there is only the induced beam-splitter interaction between two mechanical oscillators, we can obtain the enhancement of entanglement and symmetric steering by manipulating the jumping rate and feedback. Through modulating the jumping phase between cavities, we can obtain the parametric-type interaction which further improves the entanglement and steering; furthermore, the manipulable asymmetric steering can be reached. Based on the reduction of effective decay rate for the cavity mode, we have presented the generation of the steady-state and dynamical entanglement and steering under the unresolved-sideband regime, which is friendly for the experimental implementation in the view of relaxing the requirement for the optical quality factor.

APPENDIX A: THE DRIFT AND DIFFUSION MATRICES

The time-dependent drift matrix $M(t)$ in Eq. (12) is given by

$$M(t) = \begin{bmatrix} m_{a_1} & m_{12} & m_{ab}(t) & m_{ab}(t) \\ m_{21} & m_{a_2} & \mathbf{0}_2 & \mathbf{0}_2 \\ m_{ba}(t) & \mathbf{0}_2 & m_{b_1} & \mathbf{0}_2 \\ m_{ba}(t) & \mathbf{0}_2 & \mathbf{0}_2 & m_{b_2} \end{bmatrix}, \quad (A1)$$

where $\mathbf{0}_2$ is a 2×2 full-zero matrix, and $m_{a_j} = \begin{bmatrix} -\kappa_j & 0 \\ 0 & -\kappa_j \end{bmatrix}$, $m_{b_1} = \begin{bmatrix} -\gamma_1 & \Omega_1 \\ -\Omega_1 & -\gamma_1 \end{bmatrix}$, $m_{b_2} = \begin{bmatrix} -\gamma_2 & \Omega_2 \\ -\Omega_2 & -\gamma_2 \end{bmatrix}$,

$$m_{12} = \begin{bmatrix} J\sin(\theta) + 2R\sqrt{\kappa_1\kappa_2} & J\cos(\theta) \\ -J\cos(\theta) & J\sin(\theta) + 2R\sqrt{\kappa_1\kappa_2} \end{bmatrix},$$

$$m_{21} = \begin{bmatrix} -J\sin(\theta) & J\cos(\theta) \\ -J\cos(\theta) & -J\sin(\theta) \end{bmatrix},$$

$$m_{ab}(t) = \begin{bmatrix} 2\text{Im}[G(t)] & 0 \\ -2\text{Re}[G(t)] & 0 \end{bmatrix},$$

$$m_{ba}(t) = \begin{bmatrix} 0 & 0 \\ -2\text{Re}[G(t)] & -2\text{Im}[G(t)] \end{bmatrix}.$$

Under the RWA, the time-independent drift matrix M_0 can be obtained according to Eqs. (5) and (6) and is given by

$$M_0 = \begin{bmatrix} m_{a_1} & m_{12} & \bar{m}_{ab} & \bar{m}_{ab} \\ m_{21} & m_{a_2} & \mathbf{0}_2 & \mathbf{0}_2 \\ \bar{m}_{ab} & \mathbf{0}_2 & \bar{m}_{b_1} & \mathbf{0}_2 \\ \bar{m}_{ab} & \mathbf{0}_2 & \mathbf{0}_2 & \bar{m}_{b_2} \end{bmatrix}, \quad \text{(A2)}$$

where $\bar{m}_{b_1} = \begin{bmatrix} -\gamma_1 & \delta \\ -\delta & -\gamma_1 \end{bmatrix}$, $\bar{m}_{b_2} = \begin{bmatrix} -\gamma_2 & -\delta \\ \delta & -\gamma_2 \end{bmatrix}$,

$$\bar{m}_{ab} = \begin{bmatrix} 0 & G_1 - G_2 \\ -(G_1 + G_2) & 0 \end{bmatrix}.$$

The vector of input noise operators N is given by

$$N = \left[\sqrt{2\kappa_1}A_x^{(\text{in})}, \sqrt{2\kappa_1}A_y^{(\text{in})}, \sqrt{2\kappa_2}X_{a_2}^{(\text{in})}, \sqrt{2\kappa_2}P_{a_2}^{(\text{in})}, \right.$$
$$\left. \sqrt{2\gamma_1}X_{b_1}^{(\text{in})}, \sqrt{2\gamma_1}P_{b_1}^{(\text{in})}, \sqrt{2\gamma_2}X_{b_2}^{(\text{in})}, \sqrt{2\gamma_2}P_{b_2}^{(\text{in})} \right]^T, \quad \text{(A3)}$$

where the modified amplitude and phase noise operators of cavity mode a_1 are

$$A_x^{(\text{in})} = TX_{a_1}^{(\text{in})} - RX_{a_2}^{(\text{in})},$$
$$A_y^{(\text{in})} = TP_{a_1}^{(\text{in})} - RP_{a_2}^{(\text{in})}. \quad \text{(A4)}$$

Here $X_o^{(\text{in})} = (o_{\text{in}} + o_{\text{in}}^\dagger)/\sqrt{2}$ and $P_o^{(\text{in})} = (o_{\text{in}} - o_{\text{in}}^\dagger)/\sqrt{2}i$ ($o = a_j, b_j$ and $j = 1, 2$) are the input noise operators of X_o and P_o, respectively.

The diffusion matrix D is

$$D = \begin{bmatrix} d_{a_1} & d_{12} \\ d_{12} & d_{a_2} \end{bmatrix} \oplus \begin{bmatrix} d_{b_1} & \mathbf{0}_2 \\ \mathbf{0}_2 & d_{b_2} \end{bmatrix}, \quad \text{(A5)}$$

where $d_{a_j} = \kappa_j \mathbf{I}_2$, $d_{12} = -R\sqrt{\kappa_1\kappa_2}\mathbf{I}_2$, $d_{b_j} = \gamma_j(2n_{j,\text{th}} + 1)\mathbf{I}_2$.

APPENDIX B: THE REALIZATION OF THE COMPLEX COUPLING

We present a scheme to derive the complex coupling between two Fabry-Pérot cavities. We insert an auxiliary two-mode cavity between cavity a_1 and cavity a_2 (see Fig. 1), where the two-mode cavity interacts with a flying ∇-type three-level atom, shown in Fig. 7. The three-level atom is driven by a strong classical field, and two modes $\tilde{a}_1$, $\tilde{a}_2$ of the auxiliary cavity interact with atomic transition $|1\rangle \leftrightarrow |3\rangle$ and $|1\rangle \leftrightarrow |2\rangle$, respectively, where $\tilde{a}_{1,2} = \sqrt{\kappa'_{1,2}}a_{1,2}$ and κ'_1 (κ'_2) is
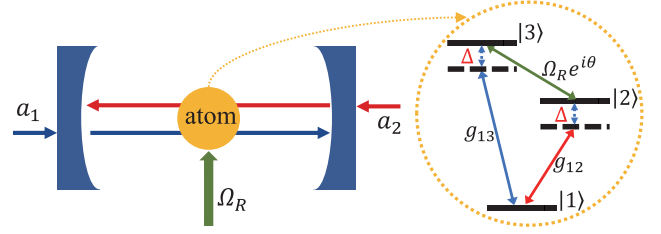

FIG. 7. Schematic diagram of the atom-cavity coupling to derive the complex coupling. A strong classical field drives the atomic transition $|2\rangle \leftrightarrow |3\rangle$, and two modes of the cavity fields interact with atomic transition $|1\rangle \leftrightarrow |3\rangle$ and $|1\rangle \leftrightarrow |2\rangle$, respectively. The circular dashed frame shows the energy-level configuration of the three-level atom.

the tunneling rate of the right (left) cavity mirror. To simplify, we write $\tilde{a}_{1,2}$ as $a_{1,2}$, and the Hamiltonian of the atom-cavity coupling system reads

$$H = \sum_{j=1,2} \omega_j a_j^\dagger a_j + E_2|2\rangle\langle2| + E_3|3\rangle\langle3| + (g_{13}a_1|3\rangle\langle1|$$
$$+ g_{12}a_2|2\rangle\langle1| + \Omega_R e^{i\theta}|3\rangle\langle2|e^{-i\omega_d t} + \text{H.c.}), \quad \text{(B1)}$$

where ω_j is the resonant frequency of the cavity mode a_j, $g_{13}(g_{12})$ represents the coupling strength between the transition $|1\rangle \to |3\rangle(|1\rangle \to |2\rangle)$ and the cavity mode $a_1(a_2)$, and Ω_R is the Rabi frequency of the classical field with frequency ω_d and phase θ. In a rotating frame with respect to $H_0 = (E_2 + \omega_d)(a_1^\dagger a_1 + |3\rangle\langle3|) + E_2(a_2^\dagger a_2 + |2\rangle\langle2|)$, the Hamiltonian of the system becomes

$$H' = \sum_{j=1,2} \Delta_j a_j^\dagger a_j + \Delta|3\rangle\langle3| + \Omega_R(e^{i\theta}|3\rangle\langle2| + e^{-i\theta}|2\rangle\langle3|)$$
$$+ (g_{13}a_1|3\rangle\langle1| + g_{12}a_2|2\rangle\langle1| + \text{H.c.}), \quad \text{(B2)}$$

where $\Delta_1 = \omega_1 - E_2 - \omega_d$, $\Delta_2 = \omega_2 - E_2$ and $\Delta = E_3 - E_2 - \omega_d$. Under the condition $\Omega_R \gg \{g_{12}, g_{13}\}$, we can obtain the dressed states that are expressed in terms of bare states as

$$|+\rangle = \cos\varphi|3\rangle + e^{-i\theta}\sin\varphi|2\rangle,$$
$$|-\rangle = \sin\varphi|3\rangle - e^{-i\theta}\cos\varphi|2\rangle, \quad \text{(B3)}$$

where $\cos\varphi = \sqrt{(d + \Delta)/2d}$, $\sin\varphi = \sqrt{(d - \Delta)/2d}$ with $d = \sqrt{4\Omega_R^2 + \Delta^2}$. The dressed states $|+\rangle, |-\rangle$ have their eigenvalues $\lambda_\pm = \frac{1}{2}(d \pm \Delta)$, respectively. Therefore, the first line of the Hamiltonian (B2) becomes $H'_0 = \sum_{j=1,2} \Delta_j a_j^\dagger a_j + \lambda_+|+\rangle\langle+| + \lambda_-|-\rangle\langle-|$. In the rotating frame with respect to H'_0, we can obtain the Hamiltonian in the interaction picture:

$$H_{\text{int}} = |+\rangle\langle1|(g_{13}\cos\varphi e^{i(\lambda_+ - \Delta_1)t}a_1$$
$$+ g_{12}\sin\varphi e^{i\theta} e^{i(\lambda_+ - \Delta_2)t}a_2)$$
$$+ |-\rangle\langle1|(g_{13}\sin\varphi e^{i(\lambda_- - \Delta_1)t}a_1$$
$$- g_{12}\cos\varphi e^{i\theta} e^{i(\lambda_- - \Delta_2)t}a_2) + \text{H.c.} \quad \text{(B4)}$$

Under the condition $(\lambda_\pm - \Delta_{1,2}) \gg \{g_{12}\sin\varphi, g_{12}\cos\varphi, g_{13}\sin\varphi, g_{13}\cos\varphi\}$, we can derive the Hamiltonian of the two-mode field $H_{\text{eff}} = -iH_{\text{int}}(t)\int_0^t ds H_{\text{int}}(s)$ when the atom collapses to a certain

energy level after the measurement. For example, when the atom collapses to the level $|1\rangle$, we can obtain

$$H_{\text{eff}} = \sum_{j=1,2} \omega_{a_j} a_j^\dagger a_j + J(e^{i\theta} a_1^\dagger a_2 + e^{-i\theta} a_2^\dagger a_1), \quad \text{(B5)}$$

with coefficients

$$\omega_{a_1} = g_{13}^2 \left[\frac{\cos^2\varphi}{\Delta - \lambda_+} + \frac{\sin^2\varphi}{\Delta - \lambda_-} \right],$$

$$\omega_{a_2} = g_{12}^2 \left[\frac{\sin^2\varphi}{\Delta - \lambda_+} + \frac{\cos^2\varphi}{\Delta - \lambda_-} \right],$$

$$J = g_{12}g_{13} \frac{\sin\varphi\cos\varphi(\lambda_+ - \lambda_-)}{(\Delta - \lambda_+)(\Delta - \lambda_-)}, \quad \text{(B6)}$$

where $\Delta_1 = \Delta_2 = \Delta$ is assumed to simplify. Therefore, the complex coupling between two cavities is constructed and the phase θ is inherited from the classical field [79].

The complex coupling between two cavities also can be generated by the time-dependent exchange coupling which has been investigated theoretically [81–83] and realized experimentally [84]. The Hamiltonian can be written as

$$H = \omega_c a_1^\dagger a_1 + (\omega_c + \Delta_{\text{opt}}) a_2^\dagger a_2$$
$$+ 2J\cos(\Delta_{\text{opt}} t + \theta)(a_1^\dagger a_2 + a_2^\dagger a_1). \quad \text{(B7)}$$

In the rotating frame with respect to $H_0 = \Delta_{\text{opt}} a_2^\dagger a_2$, the Hamiltonian becomes

$$H = \omega_c(a_1^\dagger a_1 + a_2^\dagger a_2) + J(e^{i\theta} a_1^\dagger a_2 + a_2^\dagger a_1 e^{-i\theta})$$
$$+ J(e^{-i(2\Delta_{\text{opt}} t + \theta)} a_1^\dagger a_2 + a_2^\dagger a_1 e^{i(2\Delta_{\text{opt}} t + \theta)}). \quad \text{(B8)}$$

Under the condition $2\Delta_{\text{opt}} \gg J$, the high-frequency oscillating terms can be neglected and the Hamiltonian becomes

$$H = \omega_c(a_1^\dagger a_1 + a_2^\dagger a_2) + J(e^{i\theta} a_1^\dagger a_2 + a_2^\dagger a_1 e^{-i\theta}). \quad \text{(B9)}$$

Thus, the phase-dependent coupling between two cavities is achieved.

[1] S. L. Braunstein and P. van Loock, Rev. Mod. Phys. **77**, 513 (2005).

[2] R. Horodecki, P. Horodecki, M. Horodecki, and K. Horodecki, Rev. Mod. Phys. **81**, 865 (2009).

[3] C. Harney and S. Pirandola, PRX Quantum **3**, 010311 (2022).

[4] J. Li, S.-Y. Zhu, and G. S. Agarwal, Phys. Rev. Lett. **121**, 203601 (2018).

[5] S.-S. Zheng, F.-X. Sun, H.-Y. Yuan, Z. Ficek, Q.-H. Gong, and Q.-Y. He, Sci. China Phys. Mech. Astron. **64**, 210311 (2020).

[6] Y.-F. Jiao, S.-D. Zhang, Y.-L. Zhang, A. Miranowicz, L.-M. Kuang, and H. Jing, Phys. Rev. Lett. **125**, 143605 (2020).

[7] W. Qin, A. Miranowicz, H. Jing, and F. Nori, Phys. Rev. Lett. **127**, 093602 (2021).

[8] E. Rosenfeld, R. Riedinger, J. Gieseler, M. Schuetz, and M. D. Lukin, Phys. Rev. Lett. **126**, 250505 (2021).

[9] J. Li and S. Gröblacher, Quantum Sci. Technol. **6**, 024005 (2021).

[10] H. Tan and J. Li, Phys. Rev. Res. **3**, 013192 (2021).

[11] J. Li, Y.-P. Wang, W.-J. Wu, S.-Y. Zhu, and J. Q. You, PRX Quantum **2**, 040344 (2021).

[12] D. Kong, J. Xu, Y. Tian, F. Wang, and X. Hu, Phys. Rev. Res. **4**, 013084 (2022).

[13] G. Andersson, S. W. Jolin, M. Scigliuzzo, R. Borgani, M. O. Tholén, J. C. Rivera Hernández, V. Shumeiko, D. B. Haviland, and P. Delsing, PRX Quantum **3**, 010312 (2022).

[14] M. Asjad, S. Zippilli, and D. Vitali, Phys. Rev. A **93**, 062307 (2016).

[15] C.-G. Liao, R.-X. Chen, H. Xie, M.-Y. He, and X.-M. Lin, Phys. Rev. A **99**, 033818 (2019).

[16] C.-H. Bai, D.-Y. Wang, S. Zhang, S. Liu, and H.-F. Wang, Adv. Quantum Tech. **4**, 2000149 (2021).

[17] F. Fröwis, P. Sekatski, W. Dür, N. Gisin, and N. Sangouard, Rev. Mod. Phys. **90**, 025004 (2018).

[18] I. Pikovski, M. R. Vanner, M. Aspelmeyer, M. S. Kim, and c. Brukner, Nat. Phys. **8**, 393 (2012).

[19] C. Pfister, J. Kaniewski, M. Tomamichel, A. Mantri, R. Schmucker, N. McMahon, G. Milburn, and S. Wehner, Nat. Commun. **7**, 13022 (2016).

[20] F. Massel, Phys. Rev. A **95**, 063816 (2017).

[21] M. Rossi, D. Mason, J. Chen, Y. Tsaturyan, and A. Schliesser, Nature (London) **563**, 53 (2018).

[22] F. Massel, Phys. Rev. A **100**, 023824 (2019).

[23] L. Zhou, Y. Han, J. Jing, and W. Zhang, Phys. Rev. A **83**, 052117 (2011).

[24] M. J. Woolley and A. A. Clerk, Phys. Rev. A **89**, 063805 (2014).

[25] J.-Q. Liao, Q.-Q. Wu, and F. Nori, Phys. Rev. A **89**, 014302 (2014).

[26] S. Chakraborty and A. K. Sarma, Phys. Rev. A **97**, 022336 (2018).

[27] J. F. Poyatos, J. I. Cirac, and P. Zoller, Phys. Rev. Lett. **77**, 4728 (1996).

[28] A. R. R. Carvalho, P. Milman, R. L. de Matos Filho, and L. Davidovich, Phys. Rev. Lett. **86**, 4988 (2001).

[29] L. Tóth, N. Bernier, A. Nunnenkamp, A. Feofanov, and T. Kippenberg, Nat. Phys. **13**, 787 (2017).

[30] S. Zippilli and D. Vitali, Phys. Rev. Lett. **126**, 020402 (2021).

[31] P. Zapletal, A. Nunnenkamp, and M. Brunelli, PRX Quantum **3**, 010301 (2022).

[32] J. Li, I. M. Haghighi, N. Malossi, S. Zippilli, and D. Vitali, New J. Phys. **17**, 103037 (2015).

[33] R. Riedinger, A. Wallucks, I. Marinković, C. Löschnauer, M. Aspelmeyer, S. Hong, and S. Gröblacher, Nature (London) **556**, 473 (2018).

[34] C. F. Ockeloen-Korppi, E. Damskägg, J.-M. Pirkkalainen, M. Asjad, A. A. Clerk, F. Massel, M. J. Woolley, and M. A. Sillanpää, Nature (London) **556**, 478 (2018).

[35] S. Kotler, G. A. Peterson, E. Shojaee, F. Lecocq, K. Cicak, A. Kwiatkowski, S. Geller, S. Glancy, E. Knill, R. W. Simmonds et al., Science **372**, 622 (2021).

[36] L. M. de Lépinay, C. F. Ockeloen-Korppi, M. J. Woolley, and M. A. Sillanpää, Science **372**, 625 (2021).

[37] Y. Luo and H. Tan, Quantum Sci. Technol. **5**, 045023 (2020).

[38] S. Qin, X. Xin, S. He, and C. Li, J. Opt. Soc. Am. B **38**, 3902 (2021).

[39] Y. Zhou, X. Jia, F. Li, J. Yu, C. Xie, and K. Peng, Sci. Rep. **5**, 11132 (2015).

[40] J. Li, G. Li, S. Zippilli, D. Vitali, and T. Zhang, Phys. Rev. A **95**, 043819 (2017).

[41] A. Harwood, M. Brunelli, and A. Serafini, Phys. Rev. A **103**, 023509 (2021).

[42] M. S. Ebrahimi, S. Zippilli, and D. Vitali, Quantum Sci. Technol. **7**, 035003 (2022).

[43] M. Rossi, N. Kralj, S. Zippilli, R. Natali, A. Borrielli, G. Pandraud, E. Serra, G. Di Giuseppe, and D. Vitali, Phys. Rev. Lett. **119**, 123603 (2017).

[44] L. Qiu, G. Huang, I. Shomroni, J. Pan, P. Seidler, and T. J. Kippenberg, PRX Quantum **3**, 020309 (2022).

[45] H. M. Wiseman and G. J. Milburn, Phys. Rev. A **49**, 4110 (1994).

[46] S. Lloyd, Phys. Rev. A **62**, 022108 (2000).

[47] J. Zhang, Y.-x. Liu, R.-B. Wu, K. Jacobs, and F. Nori, Phys. Rep. **679**, 1 (2017).

[48] M. D. Reid, P. D. Drummond, W. P. Bowen, E. G. Cavalcanti, P. K. Lam, H. A. Bachor, U. L. Andersen, and G. Leuchs, Rev. Mod. Phys. **81**, 1727 (2009).

[49] D. Cavalcanti and P. Skrzypczyk, Rep. Prog. Phys. **80**, 024001 (2016).

[50] S. Armstrong, M. Wang, R. Y. Teh, Q. Gong, Q. He, J. Janousek, H.-A. Bachor, M. D. Reid, and P. K. Lam, Nat. Phys. **11**, 167 (2015).

[51] Y. Xiang, I. Kogias, G. Adesso, and Q. He, Phys. Rev. A **95**, 010101(R) (2017).

[52] I. Kogias, Y. Xiang, Q. He, and G. Adesso, Phys. Rev. A **95**, 012315 (2017).

[53] C.-M. Li, K. Chen, Y.-N. Chen, Q. Zhang, Y.-A. Chen, and J.-W. Pan, Phys. Rev. Lett. **115**, 010402 (2015).

[54] Q. He, L. Rosales-Zárate, G. Adesso, and M. D. Reid, Phys. Rev. Lett. **115**, 180502 (2015).

[55] M. D. Reid, Phys. Rev. A **88**, 062338 (2013).

[56] M. Piani and J. Watrous, Phys. Rev. Lett. **114**, 060404 (2015).

[57] H. M. Wiseman, S. J. Jones, and A. C. Doherty, Phys. Rev. Lett. **98**, 140402 (2007).

[58] V. Händchen, T. Eberle, S. Steinlechner, A. Samblowski, T. Franz, R. F. Werner, and R. Schnabel, Nat. Photonics **6**, 596 (2012).

[59] Z. Qin, X. Deng, C. Tian, M. Wang, X. Su, C. Xie, and K. Peng, Phys. Rev. A **95**, 052114 (2017).

[60] C.-G. Liao, H. Xie, R.-X. Chen, M.-Y. Ye, and X.-M. Lin, Phys. Rev. A **101**, 032120 (2020).

[61] S. Zheng, F. Sun, Y. Lai, Q. Gong, and Q. He, Phys. Rev. A **99**, 022335 (2019).

[62] H. Mabuchi, Phys. Rev. A **78**, 032323 (2008).

[63] E. X. DeJesus and C. Kaufman, Phys. Rev. A **35**, 5288 (1987).

[64] G. Vidal and R. F. Werner, Phys. Rev. A **65**, 032314 (2002).

[65] M. B. Plenio, Phys. Rev. Lett. **95**, 090503 (2005).

[66] I. Kogias, A. R. Lee, S. Ragy, and G. Adesso, Phys. Rev. Lett. **114**, 060403 (2015).

[67] C. Yang, X. Wei, J. Sheng, and H. Wu, Nat. Commun. **11**, 4656 (2020).

[68] P. Piergentili, L. Catalini, M. Bawaj, S. Zippilli, N. Malossi, R. Natali, D. Vitali, and G. D. Giuseppe, New J. Phys. **20**, 083024 (2018).

[69] X. Wei, J. Sheng, C. Yang, Y. Wu, and H. Wu, Phys. Rev. A **99**, 023851 (2019).

[70] J. Sheng, X. Wei, C. Yang, and H. Wu, Phys. Rev. Lett. **124**, 053604 (2020).

[71] J. Sheng, C. Yang, and H. Wu, Sci. Adv. **7**, eabl7740 (2021).

[72] P. Piergentili, R. Natali, D. Vitali, and G. Di Giuseppe, Photonics **9**, 99 (2022).

[73] J. D. Thompson, B. M. Zwickl, A. M. Jayich, F. Marquardt, S. M. Girvin, and J. G. E. Harris, Nature (London) **452**, 72 (2008).

[74] J. C. Sankey, C. Yang, B. M. Zwickl, A. M. Jayich, and J. G. E. Harris, Nat. Phys. **6**, 707 (2010).

[75] C. Gärtner, J. P. Moura, W. Haaxman, R. A. Norte, and S. Gröblacher, Nano Lett. **18**, 7171 (2018).

[76] K.-K. Law, Opt. Lett. **19**, 607 (1994).

[77] Y. Chen, Y.-L. Zhang, Z. Shen, C.-L. Zou, G.-C. Guo, and C.-H. Dong, Phys. Rev. Lett. **126**, 123603 (2021).

[78] P. Kok, W. J. Munro, K. Nemoto, T. C. Ralph, J. P. Dowling, and G. J. Milburn, Rev. Mod. Phys. **79**, 135 (2007).

[79] N. A. Ansari, J. Gea-Banacloche, and M. S. Zubairy, Phys. Rev. A **41**, 5179 (1990).

[80] G.-L. Schmid, C. T. Ngai, M. Ernzer, M. B. Aguilera, T. M. Karg, and P. Treutlein, Phys. Rev. X **12**, 011020 (2022).

[81] B. Peropadre, D. Zueco, F. Wulschner, F. Deppe, A. Marx, R. Gross, and J. J. García-Ripoll, Phys. Rev. B **87**, 134504 (2013).

[82] K. Fang, Z. Yu, and S. Fan, Nat. Photonics **6**, 782 (2012).

[83] D. Porras and S. Fernández-Lorenzo, Phys. Rev. Lett. **122**, 143901 (2019).

[84] P. Roushan, C. Neill, A. Megrant, Y. Chen, R. Babbush, R. Barends, B. Campbell, Z. Chen, B. Chiaro, A. Dunsworth *et al.*, Nat. Phys. **13**, 146 (2017).

[85] J. W. Rao, S. Kaur, B. M. Yao, E. R. J. Edwards, Y. T. Zhao, X. Fan, D. Xue, T. J. Silva, Y. S. Gui, and C.-M. Hu, Nat. Commun. **10**, 2934 (2019).

[86] J. Kerckhoff and K. W. Lehnert, Phys. Rev. Lett. **109**, 153602 (2012).

[87] L.-M. Duan, G. Giedke, J. I. Cirac, and P. Zoller, Phys. Rev. Lett. **84**, 2722 (2000).

[88] T. A. Palomaki, J. D. Teufel, R. W. Simmonds, and K. W. Lehnert, Science **342**, 710 (2013).